Published in final edited form as:
Glia. 2009 August 15; 57(11): 1239–1249. doi:10.1002/glia.20845.

Microarray analyses reveal regional astrocyte heterogeneity with implications for neurofibromatosis type 1 (NF1)-regulated glial proliferation

Tu-Hsueh Yeh[1,2], **Da Yong Lee**[1], **Scott M. Gianino**[1], and **David H. Gutmann**[1]

[1] Department of Neurology, Washington University School of Medicine, St. Louis MO

[2] Department of Neurology, Chang Gung Memorial Hospital and University, Taipei, Taiwan

Abstract

Numerous studies have suggested that astrocytes in the central nervous system (CNS) exhibit molecular and functional heterogeneity. In this regard, astrocytes from different CNS locations express distinct immune system and neurotransmitter proteins, have varying levels of gap junction coupling, and respond differently to injury. However, the relevance of these differences to human disease is unclear. Since brain tumors in children arise in specific CNS locations, we hypothesized that regional astrocyte heterogeneity might partly underlie the propensity for gliomas to arise in these areas. In this study, we performed high-density RNA microarray profiling on astrocytes from postnatal day 1 optic nerve, cerebellum, brainstem, and neocortex. We showed that astrocytes from each region are molecularly distinct, and we were able to develop gene expression patterns that distinguish astrocytes, but not neural stem cells, from these different brain regions. We next used these microarray data to determine whether brain tumor suppressor genes were differentially expressed in these distinct populations of astrocytes. Interestingly, neurofibromatosis type 1 (NF1) gene expression was decreased at both the RNA and protein levels in neocortical astrocytes relative to astrocytes from the other brain regions. To determine the functional significance of this finding, we found increased astrocyte proliferation in optic nerve, brainstem, and cerebellum, but not neocortex, following *Nf1* inactivation *in vitro* and *in vivo*. These findings provide molecular evidence for CNS astrocyte heterogeneity, and suggest that differences in tumor suppressor gene expression might contribute to the regional localization of human brain tumors.

Keywords

neurofibromin; NG2; inherited cancer syndrome; astrocytoma

Introduction

Brain tumors in children typically occur in specific brain regions, both sporadically and in the context of inherited cancer syndromes. In this regard, histologic subtypes of glial cell tumors (astrocytomas) frequent arise in certain locations within the neuraxis. For example, 98% of pleiomorphic xanthoastrocytomas, a World Health Organization (WHO) grade II glial neoplasm, arise supratentorially and tend to involve the temporal lobes (Giannini et al. 2002), whereas pilomyxoid astrocytomas, another pediatric low-grade glioma, most frequently are located within the hypothalamus and optic chiasm (Ceppa et al. 2007; Fernandez et al. 2003). Similarly, over half of dysembryoplastic neuroepithelial tumors are

Corresponding author: David H. Gutmann, MD, PhD, Department of Neurology, Washington University School of Medicine, Box 8111; 660 South Euclid Avenue, St. Louis MO 63110. Email (gutmannd@wustl.edu).

found in the temporal lobe (Daumas-Duport 1993; Honavar et al. 1999; Prayson and Estes 1992).

In addition, glial cell neoplasms arising in inherited tumor predisposition syndromes also show specific regional distributions. In contrast to sporadic WHO grade I pilocytic astrocytomas which are most frequently located in the cerebellum (Malik et al. 2006; Ohgaki and Kleihues 2005), two-thirds of brain tumors in individuals with neurofibromatosis type 1 (NF1) arise in the optic pathway (optic nerve, optic chiasm, and optic radiations) (Guillamo et al. 2003). In addition, the vast majority of glial tumors in the neurofibromatosis type 2 (NF2) inherited cancer syndrome are ependymomas that arise within the spinal cord (Rodriguez and Berthrong 1966).

While these unique patterns of brain tumor formation may reflect the presence of specific stromal (microenvironmental) signals unique to these brain locations, it is also possible that glial cells (astrocytes) from different brain regions are genetically distinct, and that this molecular diversity partly dictates the response of tumor-generating cells to specific tumor-causing genetic changes. To gain insights into the molecular heterogeneity of CNS astrocytes, we performed high-density Affymetrix RNA microarray analyses on astrocytes from four brain regions in which tumors arise in children (cerebellum, optic nerve, brainstem, and neocortex), and demonstrated that astrocytes from each CNS region are molecularly distinct. Based on these microarray results, we were able to develop gene expression patterns that distinguish astrocytes, but not neural stem cells, from these different brain locations. To determine the relevance of this molecular heterogeneity to brain tumors, we examined the differential expression of tumor suppressor genes in these distinct populations of astrocytes and found that *Nf1* mRNA and protein expression was decreased in neocortical astrocytes relative to astrocytes from the other regions. Moreover, we found that *Nf1* inactivation resulted in increased proliferation of astrocytes from optic nerve, brainstem, and cerebellum, but not neocortex, *in vitro* and *in vivo*.

Materials and Methods

Mice

Nf1$^{flox/flox}$ (Zhu et al. 2001) and *Nf1*^{GFAP}CKO (Bajenaru et al. 2002) mice were generated as previously described and maintained on a C57Bl/6 background. All mice were used in accordance with approved Animal Studies Protocols.

Primary astroglial cultures

Murine astroglial cultures were generated from postnatal day 1 or 2 wild-type or *Nf1*$^{flox/flox}$ pups as previously described (Sandsmark et al. 2007). Briefly, fronto-parietal lobe neocortex (CTX), cerebellar hemispheres (CB) and medulla (brainstem; BS) were isolated, enzymatically digested in 0.05% trypsin for 20 min, and maintained in astrocyte growth medium (DMEM containing 10% fetal bovine serum and antibiotics). For optic nerve (ON) astroglial cell cultures, each nerve was minced and the resulting cells grown in 6-well plate for 5–7 days prior to seeding in culture flasks containing astrocyte growth medium. The *Nf1* gene was inactivated in passage 1 *Nf1*$^{flox/flox}$ astrocytes by infection with adenovirus (Ad5) containing Cre recombinase (University of Iowa Gene Transfer Vector Core, Iowa City, IA). Control *Nf1*$^{flox/flox}$ astrocytes (wild-type) were treated identically with an adenovirus encoding LacZ. Four days after Cre adenovirus treatment, neurofibromin expression was examined by Western blot. In all cases, neurofibromin expression was absent in astroglial cells infected with Ad5-Cre compared to those infected with Ad5-LacZ (data not shown). At least two to three pups were pooled for each culture.

Neural stem cell cultures

As above, CTX, CB and BS were removed from postnatal day 1 (PN1) wild-type mice and processed to obtain single-cell suspension of neural progenitors (neurospheres). Neurospheres were maintained in NSC medium on UltraLow plates (Fisher, St. Louis, MO) as previously described (Dasgupta and Gutmann 2005).

RNA isolation and microarray analysis

Total RNA was extracted from primary cultured astrocytes from CTX, CB, BS, and ON using RNeasy Mini Kit (Qiagen, Valencia, CA). RNA samples were quantified and RNA integrity was analyzed following the manufacturer's recommendations (Affymetrix, Santa Clara, CA). Target preparation and microarray hybridization were performed by the Siteman Cancer Center Multiplex Gene Analysis Core Facility using Affymetrix Mouse Genome 430 2.0 GeneChip microarrays. Basic microarray data visualization and data filtering were accomplished as previously described (Sharma et al. 2007). Fold change was calculated by dividing the average values of one region by the average values of the other regions for each probe set. Statistical significance was determined with Student's *t* test using Spotfire DecisionSite for Functional Genomics (TIBCO Spotfire, Somerville, MA). The *P* values obtained with Student's *t* test were corrected for multiple testing by the Benjamini-Hochberg method (Benjamini and Hochberg 1995). Unsupervised hierarchical clustering was performed on samples from four brain regions using the following methods: (a) clustering method: unweighted pair group method using arithmetic average (UPGMA), similarity measure: Euclidean distance; (b) clustering method: UPGMA, similarity measure: correlation. Probe sets that were absent across all chips and the Affymetrix control probe sets were filtered from the analysis. Selection of probe sets whose signals were significantly different between one region and another were prioritized for further study by the statistical test and the fold change.

Real-time reverse transcription-PCR

The expression of specific genes was examined by real-time reverse transcription-PCR (RT-PCR) using SYBR Green detection chemistry. Two micrograms of total RNA extracted from each of the samples were used tomake cDNA. Forty nanograms of cDNA were used as template for PCR amplification with primers specific for each of the transcripts examined (Supplemental Table S1). PCR reactions without cDNA samples were used as negative controls. Each reaction was performed in duplicate. SDS system software (Applied Biosystems, Foster City, CA) was used to convert the fluorescent data into cycle threshold (C_T) measurements, and the $\Delta\Delta C_T$ method (Livak and Schmittgen 2001) was used to calculate fold expression, using β-actin as an internal control. For each gene, at least three independent astrocyte cultures, NSC cultures, or brain region specimens were used.

Cell proliferation

50,000 astrocytes were plated in 24-well dishes, allowed to adhere, and maintained in serum-free DMEM for 24 h before exposure to [^{3}H]-thymidine (1 μCi/μL) for 20 h. [^{3}H]thymidine incorporation was determined by scintillation counting as previously described (Sandsmark et al. 2007). Each experiment was performed at least three times using independently-generated astroglial cell cultures.

Immunocytochemistry

Immunofluorescence staining was performed using the following primary antibodies: GFAP (Sigma; St. Louis, MO), AQP4, NG2, O4, LHX2 (Chemicon International; Temecula, CA), APC (Calbiochem; San Diego, CA), FOXG1, FOXP2 (Abcam; Cambridge, MA), HOXB3 (Santa Cruz Biotechnology; Santa Cruz, CA), and GLAST (a gift from Dr. Watanabe;

(Shibata et al. 1997)). Visualization was accomplished after incubation with either Alexa Fluor 488 or 568 secondary antibodies (Invitrogen, Eugene, OR) using an inverted Eclipse TE300 (Nikon) microscope equipped with an optical camera (Optronics). Cells were counterstained with DAPI. Quantification was performed by counting the number of immunopositive cells as a percentage of the total number of DAPI-stained nuclei in at least five randomly selected fields (>100 cells) in three independently-isolated cultures.

Immunohistochemistry

Immunohistochemical staining was performed using GFAP (Zymed, San Francisco, CA) or Ki-67 (BD Pharmingen, San Diego, CA) antibodies followed by Vectastain ABC development (Vector Laboratories, Burlingame, CA). GFAP-positive and Ki-67(MIB-1)-immunoreactive cells were quantified by direct counting of representative matched areas from each brain region at 20x objective magnification as previously described (Hegedus et al., 2008). For NG2 immunofluorescence staining, the pixel intensity was determined using image analysis software MetaMorph (Molecular Devices, Downingtown, PA), and the relative intensity calculated using the logarithm of the index value (optic nerve fluorescence signal value/background value). At least four mice were used for each experiment.

Western blot analysis

Astrocytes were serum-starved overnight, harvested by scraping in ice-cold PBS, and lysed in NP40 lysis buffer with protease inhibitors. Western blotting was performed as previously described (Dasgupta and Gutmann, 2005). Rabbit anti-NF1GRP-D (Santa Cruz Biotechnology, Santa Cruz, CA) was used at a 1:200 dilution to detect neurofibromin expression. Detection was accomplished by enhanced chemiluminescence (Amersham Biosciences, Pittsburgh, PA). α-tubulin (Sigma, St. Louis, MO) was employed for normalization and densitometric analysis using Gel-Pro Analyzer 4.0 (Media Cybernetics, Bethesda, MD).

Statistical analyses

Statistical analyses were performed using GraphPad Prism 4.0 software (GraphPad, La Jolla, CA). Student's two-tailed *t*-test was used with significance set at $P<0.05$. All *in vitro* experiments were performed at least three times with similar results.

Results

Astroglial cells from different brain regions have distinct gene expression patterns

Using Affymetrix Mouse Genome 430 2.0 GeneChip microarrays containing >39,000 transcripts and variants representing ~34,000 mouse genes, a small set of 1446 differential expressed genes (4.2% of total genes) were identified. Quantitative comparison of CTX, CB, BS, and ON gene expression allowed for the identification of all genes that met the following criteria (Supplemental Tables S2-S5): (a) enriched by at least two-fold, (b) statistically different by corrected *p*-values less than 0.05, and (c) present in at least two third of samples or absent in all samples of other regions. These included 184 CTX-enriched genes (225 probe sets, 0.54% of total genes), 47 CB-enriched genes (58 probe sets, 0.14% of total genes), 164 BS-enriched genes (171 probe sets, 0.48% of total genes), and 1051 ON-enriched genes (1314 probe sets, 3.09% of total genes). The heatmap generated from unsupervised hierarchical gene clustering using z-score normalization of expression data revealed distinct gene expression patterns that distinguish astroglial cells from these four brain regions (Figure 1A). The dendrogram showed two main branches: one containing ON astroglial cells and another tight cluster which was divided into CTX, CB and BS astroglial cell subsets.

To confirm that the cells in these cultures were astrocytes, immunocytochemical analyses using established astrocyte markers were performed. Greater than 98% of the cells from CTX, CB, and BS astroglial cultures were GFAP+. Similarly, >83% of the cells from these cultures expressed aquaporin-4 (AQP4) and the astroglial glutamate transporter GLAST (Figure 1B). In contrast, O4- or APC-positive (oligodendrocyte lineage) cells were rarely detected (Figure S1).

To further demonstrate that these cultures contained astroglial cells, we examined the microarray data for expression of astroglial-, oligodendrocyte-, microglia-, endothelial cell-, fibroblast-, and neuron-specific transcripts. Cells from all three regions expressed high levels of astrocyte-specific genes and very low levels of oligodendrocyte-, microglia-, endothelial cell-, fibroblast-, or neuron-specific genes (Figure 1C and Figure S2A & B). By immunocytochemistry, fewer than 5% of the cells in these cultures were microglia, and no fibroblasts or endothelial cells were detected (Figure S2C). Collectively, these results indicate that astroglial cells from different brain regions with identical immunomarker phenotypes are genetically distinct.

Identification and validation of genes differentially expressed in neocortex, cerebellum and brainstem

To independently validate these region-specific gene expression patterns, we analyzed mRNA expression of four representative candidate genes for each region by quantitative real-time RT-PCR assay in independently-generated sets of samples (Figure 2A). Consistent with the microarray data, we observed increased *Atp1a2*, *Foxg1*, *Lhx2* and *Nr2e1* expression in CTX astrocytes, increased *En2*, *Pax*, *Ptn* and *Scn7a* expression in CB astrocytes, and increased *Hoxa5*, *Hoxb3*, *Hoxb5* and *Npy* expression in BS astrocytes (Figure 2B). At the protein level, we examined LHX2, FOXG1 and HOXB3 by immunocytochemistry and found similar patterns of brain region-specific astroglial cell expression (Figure S3B).

To determine whether these region-specific gene expression patterns are retained in astroglial progenitor cells, we examined the mRNA expression of these region-enriched genes in neural stem cells (NSCs). Quantitative RT-PCR showed a similar differential gene expression pattern in NSCs from CTX; however, the region-specific gene expression patterns were not retained in NSCs from CB or BS (Figure 2C). Next, we sought to determine these gene expression profiles were also found in whole tissue from the three different brain regions. Similar to what we observed with NSCs, the region-specific gene expression patterns were not completely retained in brain tissue from these different regions (Figure 2D). Collectively, these findings suggest that these molecular signatures most accurately distinguish astroglial cells, but not other cell types, from different brain regions.

Optic nerve astroglial cells are a molecularly and genetically distinct glial subtype

As demonstrated by the distinct gene expression pattern of ON astroglial cells relative to CTX, CB or BS astroglial cells (Figure 1A), we next sought to better characterize this unique population of ON cells. We first examined these cultures for the expression of known glial cell proteins. In contrast to astroglial cells from CB, CTX, and BS, ~30% of these cells expressed GFAP, AQP4 or GLAST. Interestingly, ~70% of cells expressed the NG2 chondroitin sulphate proteoglycan (Figure 3A). It is important to note that there was mutually exclusive expression of NG2 and GFAP in these astroglial cells. Since some studies have suggested that NG2 is a marker for oligodendrocyte precursor cells (OPCs) (Levine et al., 2001), we examined the expression of two common OPC markers, O4 and APC, and found no expression of either O4 or APC in these ON astroglial cell cultures (Figure S1). Moreover, mRNA expression of two additional OPC-associated genes, *Pdgfra* and *Cd9*, was not increased in ON astroglial cell cultures compared to astroglial cells from

the other brain regions (Figure S4A & B). In addition, we analyzed the microarray data for oligodendroglial lineage markers. Whereas we observed high levels of *Cspg4* (NG2) expression in ON astroglial cell cultures, very low mRNA levels of the *Sox10*, *Mag* and *Mog* oligodendrocyte-associated genes were detected (Figure 3B), suggesting the majority of cells in ON cultures were NG2+ glia.

Among the 1051 differentially expressed genes, we examined mRNA expression of four representative genes by quantitative real-time RT-PCR (Figure 3C). Consistent with the RNA microarray results, *Foxp2*, *Grb10*, *Npr3* and *Sdpr* expression was significantly higher in ON astroglial cell culture compared to astroglial cell cultures from the other brain regions (Figure 3D). In addition, FOXP2 immunocytochemistry revealed that >90% positive of ON astroglial cells expressed FOXP2 compared to <10% of the astroglial cells from CTX, CB and BS (Figure S3B). In contrast to the results obtained with region-specific BS, CB, and CTX genes, the ON-specific gene expression pattern was also observed in optic nerve tissue compared with tissue from different brain regions (Figure 3E). Unfortunately, multipotent NSCs could not be isolated from PN1 mouse optic nerve for analysis (D.Y.L. & D.H.G., unpublished observations).

Differential brain region expression of glioma-associated tumor suppressor genes

Since brain tumors tend to arise in specific brain regions, we next sought to determine whether differential patterns of glioma tumor suppressor gene expression might exist. In our genome-wide gene expression analysis of astroglial cells from different brain regions, we found that several tumor suppressor genes related to gliomagenesis showed a region-specific differential expression pattern (Table 1). The vast majority of these genes showed fold changes that were unlikely to be biologically significant. Notably, only one gene demonstrated highly significant differential gene expression: Neurofibromatosis type 1 (NF1) mRNA expression in CB, BS and ON astroglial cells was between 2- and 4.6-fold higher relative to astroglial cells from CTX.

To confirm these microarray results, we performed quantitative real-time RT-PCR using *Nf1*-specific primers. Significantly higher levels of *Nf1* mRNA expression were observed in astroglial cells from ON, CB and BS compared to CTX (Figure 4A). In addition, Western blot analysis also demonstrated significantly lower levels of neurofibromin expression in CTX astroglial cells than in astroglial cells from the other brain regions (Figure 4B). Since NF1-associated brain tumor uncommonly arise in the cortex, this differential pattern of *Nf1* gene expression might impact on astroglial cell proliferation and gliogenesis.

Neocortical astroglial cells exhibit no change in proliferation in response to Nf1 inactivation in vitro or in vivo

To provide functional support for the hypothesis that the differential pattern of neurofibromin expression might result in differences in astroglial cell growth following *Nf1* loss, we examined astroglial cell proliferation in response to *Nf1* inactivation *in vitro* and *in vivo*. First, we generated $Nf1^{flox/flox}$ astroglial cultures from the four different brain regions, and treated these cultures with either Ad5-Cre or Ad5-LacZ to generate $Nf1^{-/-}$ and wild-type astroglial cells, respectively. In all cases, neurofibromin levels were undetectable in astroglial cells infected with Ad5-Cre compared to Ad5-LacZ (data not shown). Next, $Nf1^{-/-}$ and wild-type astroglial cells from these brain regions were assayed for the effect of neurofibromin loss on cell proliferation. Using [^{3}H]-thymidine incorporation, *Nf1* inactivation resulted in ≥2-fold increase in proliferation of astroglial cells from CB, BS and ON (Figure 5A). In contrast, no increase in proliferation was observed following *Nf1* inactivation in CTX astroglial cells.

To provide an *in vivo* demonstration of this differential sensitivity to *Nf1* inactivation, we employed a conditional knockout approach using GFAP-Cre mice developed in our laboratory. In these mice, Cre expression is first detected by embryonic day 13.5 (Bajenaru et al., 2002). For these experiments, cohorts of $Nf1^{flox/flox}$; GFAP-Cre ($Nf1^{GFAP}$CKO) and $Nf1^{flox/flox}$ (control) mice were analyzed. Whereas there was no effect of *Nf1* loss on the number of GFAP+ cells in the CTX, we observed nearly a 2-fold increase in the number of GFAP+ cells in the BS of $Nf1^{GFAP}$CKO relative to control mice (Figure 5B & C). Similarly, we found significantly more GFAP+ cells in the CB of $Nf1^{GFAP}$CKO relative to control mice (data not shown). Since few of the astroglial cells in the optic nerve cultures were GFAP+, we chose to quantitate the number of NG2+ cells in the optic nerves from $Nf1^{GFAP}$CKO and control mice. Since we could not accurately count the number of NG2+ cells, we quantitated the relative fluorescence intensity, and detected a 50% increase in NG2 staining in the $Nf1^{GFAP}$CKO mouse optic nerves relative to the control mouse optic nerves. The lower levels of astroglial cell numbers in ON relative to BS parallel the *in vitro* proliferation results (Figure 5A).

Finally, we sought to determine the effect of *Nf1* loss on astroglial cell proliferation in these different brain regions, we performed Ki67 staining. Consistent with *in vitro* proliferation results, we observed increased numbers of Ki-67-immunoreactive cells in CB, BS and ON of $Nf1^{GFAP}$CKO mice, but not in the CTX (Figure 5C). As above, the magnitude of the increased proliferation observed in ON relative to CB and BS *in vivo* parallels what was observed *in vitro*. Collectively, these results suggest that differential brain region *Nf1* gene expression has consequences for astroglial cell proliferation *in vitro* and *in vivo*.

Discussion

Numerous studies have shown that astrocytes from different regions of the CNS have distinctive patterns of gene expression and unique biological properties. In this regard, cerebellar and optic nerve astrocytes have stronger gap junction coupling than spinal cord astrocytes (Lee et al., 1994), whereas cerebellar astrocytes exhibit the most prominent stellation in response to cyclic AMP treatment (Won and Oh, 2000). Similarly, astrocyte region-specific differences in adrenergic receptor binding sites (Ernsberger et al., 1990), preproencephalin mRNA expression (Batter and Kessler, 1991), carboxypeptidase mRNA expression (Klein and Fricker, 1992), and opioid receptor expression (Ruzicka et al., 1995) have been reported. In addition, there are regional differences in immune system molecule expression, including ICAM and IL-6, in brainstem astrocytes relative to astrocytes from the neocortex (Morga et al., 1998). In total, these studies demonstrate that there are molecular and functional differences between astrocytes from different brain regions, but they do not provide an obvious connection to human disease.

In an effort to define the molecular heterogeneity of astrocyte populations from different regions of the CNS relevant to human brain tumor formation, we employed microarray RNA expression profiling to identify molecular signatures for astrocytes from neocortex, cerebellum, optic nerve, and brainstem – brain regions in which gliomas arise. First, we found that astroglial cells from the brainstem, neocortex, and cerebellum were more closely related to each other than to astrocytes from the optic nerve. This molecular similarity was also reflected by the differential expression of GFAP in these populations. Whereas astrocytes from the brainstem, neocortex, and cerebellum contained >98% GFAP+ cells, those from the optic nerve contained fewer than 30% GFAP+ cells. Similarly, greater than 80% of the astrocytes from the brainstem, neocortex, and cerebellum expressed aquaporin-4 (AQP4) and GLAST, only one-third of the astroglial cells from the optic nerve were AQP4- or GLAST-positive. These findings are consistent with previous studies (Stallcup and

Beasley, 1987) and suggest that optic nerve astroglial cells may represent a unique population of glia-like cells.

Second, we found that the majority of optic nerve astroglial cells expressed the NG2 proteoglycan. In contrast, fewer than 5% of astrocytes from the brainstem, cerebellum, or neocortex expressed NG2. Previous studies have suggested that NG2+ cells are actually oligodendrocyte precursor cells (Chen et al., 2002): NG2+ cells can give rise to A2B5+ cells in the optic nerve, and the majority of NG2+ cells become GFAP+ cells after 5 days in culture (Stallcup and Beasley, 1987). However, we did not observe increased numbers of GFAP+ cells in our ON astroglial cells as a function of time in culture. In addition, we examined the expression of several genes associated with oligodendrocyte maturation, including O4 and APC at the protein level, and found insignificant numbers of O4+ or APC + cells in our ON astroglial cell cultures. Moreover, the mRNA expression of other oligodendrocyte/oligodendrocyte precursor-associated genes (*Pdgfra*, *Cd9*, *sox10*, *mag*, and *mog*) was not increased in ON astroglial cells relative to the other three populations of brain astrocytes.

Alternatively, it has been suggested that NG2+ cells represent a fourth neuroglial cell type in the CNS (Peters, 2004). Consistent with the idea that NG2+ cells are a distinct type of neuroglial cell, we also found that NG2+ cells were GFAP-negative, similar to previous reports. NG2+ cells in the optic nerve have been hypothesized to form a functional syncytium (Sontheimer et al., 1990), receive presynaptic input from neurons, respond to neurotransmitters release at synapses, and extend processes to contact nodes of Ranvier to facilitate axon-glial signaling (Butt et al., 2004). Further study will be required to better characterize the functional properties of these astrocytes.

Third, we identified discrete gene expression patterns unique to astrocytes from each of the four brain regions. We selected representative transcripts to validate at the RNA and protein levels by quantitative PCR and immunocytochemistry. As expected, we were able to validate these molecular signatures using independently-generated astrocyte cultures. However, we found that these signatures were unique to astrocytes, and were not always shared with neural stem cells or whole brain tissue from that specific region. These results indicate that these genetic profiles are most useful for discriminating astrocytes in these brain regions and are unlikely to reflect a global gene expression pattern specific to that CNS location. In the case of the optic nerve, we did find that the pattern of differential gene expression validated at the whole tissue level, most likely reflecting the fact that most of the RNA derives from astroglial cell bodies in the optic nerve.

To extend our findings to brain tumors, we examined the expression of known tumor suppressor genes involved in brain tumor predisposition syndromes, and found that the neurofibromatosis type 1 (NF1) gene was highly expressed in astrocytes from the brainstem, cerebellum, and optic nerve relative to those from the neocortex. The observation that neurofibromin expression was significantly lower in neocortical astrocytes is consistent with the rarity of astrocytomas arising in cortical locations in children with NF1.

The differential expression of neurofibromin in neocortical astrocytes prompted us to examine the functional consequences of *Nf1* inactivation on astrocyte proliferation *in vitro* and *in vivo*. Our finding that *Nf1* loss has a limited effect on neocortical astrocyte proliferation suggests that these astrocytes are less dependent on neurofibromin for growth regulation than astrocytes from other brain regions, and are therefore considerably less affected by *Nf1* loss. In this regard, we hypothesize that the regional specificity of astrocytoma formation in NF1 is partly dependent on intrinsic genetic programs unique to different astrocyte populations. These region-specific astrocyte gene expression patterns

result in the differential expression of critical growth regulators (e.g., tumor suppressor genes) that control glial cell proliferation or survival. In this fashion, the differential expression of growth regulatory genes restricts the response of glial cells to proliferative and survival signals that emanate from the surrounding brain. We envision that regional differences in astrocyte gene expression determine where and when astrocytomas form in concert with spatially- or temporally-restricted stromal (microenvironmental) factors (Rubin and Gutmann, 2005; Warrington et al., 2007). The notion that astrocyte heterogeneity may impact on the propensity of glial cells to undergo malignant transformation illustrates the complex interplay between the intrinsic properties of astrocytes and specific cancer-causing genetic changes relevant to brain tumorigenesis.

Supplementary Material

Refer to Web version on PubMed Central for supplementary material.

Acknowledgments

This work was supported in grants from the National Institutes of Health (NS058433-01) and National Cancer Institute (U01-CA84314) to DHG.

References

Bajenaru ML, Zhu Y, Hedrick NM, Donahoe J, Parada LF, Gutmann DH. Astrocyte-specific inactivation of the neurofibromatosis 1 gene (NF1) is insufficient for astrocytoma formation. Mol Cell Biol. 2002; 22(14):5100–13. [PubMed: 12077339]

Batter DK, Kessler JA. Region-specific regulation of preproenkephalin mRNA in cultured astrocytes. Brain Res Mol Brain Res. 1991; 11(1):65–9. [PubMed: 1722552]

Benjamini Y, Hochberg Y. Controlling the false discovery rate: a practical and powerful approach to multiple testing. J Roy Stat Soc, Ser B. 1995; 57:289–300.

Butt AM, Pugh M, Hubbard P, James G. Functions of optic nerve glia: axoglial signalling in physiology and pathology. Eye. 2004; 18(11):1110–21. [PubMed: 15534596]

Ceppa EP, Bouffet E, Griebel R, Robinson C, Tihan T. The pilomyxoid astrocytoma and its relationship to pilocytic astrocytoma: report of a case and a critical review of the entity. J Neurooncol. 2007; 81(2):191–6. [PubMed: 16850101]

Chen ZJ, Negra M, Levine A, Ughrin Y, Levine JM. Oligodendrocyte precursor cells: reactive cells that inhibit axon growth and regeneration. J Neurocytol. 2002; 31(6–7):481–95. [PubMed: 14501218]

Dasgupta B, Gutmann DH. Neurofibromin regulates neural stem cell proliferation, survival, and astroglial differentiation in vitro and in vivo. J Neurosci. 2005; 25(23):5584–94. [PubMed: 15944386]

Daumas-Duport C. Dysembryoplastic neuroepithelial tumours. Brain Pathol. 1993; 3(3):283–95. [PubMed: 8293188]

Ernsberger P, Iacovitti L, Reis DJ. Astrocytes cultured from specific brain regions differ in their expression of adrenergic binding sites. Brain Res. 1990; 517(1–2):202–8. [PubMed: 2375990]

Fernandez C, Figarella-Branger D, Girard N, Bouvier-Labit C, Gouvernet J, Paz Paredes A, Lena G. Pilocytic astrocytomas in children: prognostic factors--a retrospective study of 80 cases. Neurosurgery. 2003; 53(3):544–53. discussion 554–5. [PubMed: 12943571]

Giannini C, Scheithauer BW, Lopes MB, Hirose T, Kros JM, VandenBerg SR. Immunophenotype of pleomorphic xanthoastrocytoma. Am J Surg Pathol. 2002; 26(4):479–85. [PubMed: 11914626]

Guillamo JS, Creange A, Kalifa C, Grill J, Rodriguez D, Doz F, Barbarot S, Zerah M, Sanson M, Bastuji-Garin S, et al. Prognostic factors of CNS tumours in Neurofibromatosis 1 (NF1): a retrospective study of 104 patients. Brain. 2003; 126(Pt 1):152–60. [PubMed: 12477702]

Hegedus B, Banerjee D, Yeh TH, Rothermich S, Perry A, Rubin JB, Garbow JR, Gutmann DH. Preclinical cancer therapy in a mouse model of neurofibromatosis-1 optic glioma. Cancer Res. 2008; 68(5):1520–8. [PubMed: 18316617]

Honavar M, Janota I, Polkey CE. Histological heterogeneity of dysembryoplastic neuroepithelial tumour: identification and differential diagnosis in a series of 74 cases. Histopathology. 1999; 34(4):342–56. [PubMed: 10231402]

Klein RS, Fricker LD. Heterogeneous expression of carboxypeptidase E and proenkephalin mRNAs by cultured astrocytes. Brain Res. 1992; 569(2):300–10. [PubMed: 1540832]

Lee SH, Kim WT, Cornell-Bell AH, Sontheimer H. Astrocytes exhibit regional specificity in gap-junction coupling. Glia. 1994; 11(4):315–25. [PubMed: 7960035]

Levine JM, Reynolds R, Fawcett JW. The oligodendrocyte precursor cell in health and disease. Trends Neurosci. 2001; 24(1):39–47. [PubMed: 11163886]

Livak KJ, Schmittgen TD. Analysis of relative gene expression data using real-time quantitative PCR and the 2(-Delta Delta C(T)) Method. Methods. 2001; 25(4):402–8. [PubMed: 11846609]

Malik A, Deb P, Sharma MC, Sarkar C. Neuropathological spectrum of pilocytic astrocytoma: an Indian series of 120 cases. Pathol Oncol Res. 2006; 12(3):164–71. [PubMed: 16998597]

Morga E, Faber C, Heuschling P. Cultured astrocytes express regional heterogeneity of the immunoreactive phenotype under basal conditions and after gamma-IFN induction. J Neuroimmunol. 1998; 87(1–2):179–84. [PubMed: 9670860]

Ohgaki H, Kleihues P. Population-based studies on incidence, survival rates, and genetic alterations in astrocytic and oligodendroglial gliomas. J Neuropathol Exp Neurol. 2005; 64(6):479–89. [PubMed: 15977639]

Peters A. A fourth type of neuroglial cell in the adult central nervous system. J Neurocytol. 2004; 33(3):345–57. [PubMed: 15475689]

Prayson RA, Estes ML. Dysembryoplastic neuroepithelial tumor. Am J Clin Pathol. 1992; 97(3):398–401. [PubMed: 1543164]

Rodriguez HA, Berthrong M. Multiple primary intracranial tumors in von Recklinghausen's neurofibromatosis. Arch Neurol. 1966; 14(5):467–75. [PubMed: 4957904]

Rubin JB, Gutmann DH. Neurofibromatosis type 1 - a model for nervous system tumour formation? Nat Rev Cancer. 2005; 5(7):557–64. [PubMed: 16069817]

Ruzicka BB, Fox CA, Thompson RC, Meng F, Watson SJ, Akil H. Primary astroglial cultures derived from several rat brain regions differentially express mu, delta and kappa opioid receptor mRNA. Brain Res Mol Brain Res. 1995; 34(2):209–20. [PubMed: 8750824]

Sandsmark DK, Zhang H, Hegedus B, Pelletier CL, Weber JD, Gutmann DH. Nucleophosmin mediates mammalian target of rapamycin-dependent actin cytoskeleton dynamics and proliferation in neurofibromin-deficient astrocytes. Cancer Res. 2007; 67(10):4790–9. [PubMed: 17510408]

Sharma MK, Mansur DB, Reifenberger G, Perry A, Leonard JR, Aldape KD, Albin MG, Emnett RJ, Loeser S, Watson MA, et al. Distinct genetic signatures among pilocytic astrocytomas relate to their brain region origin. Cancer Res. 2007; 67(3):890–900. [PubMed: 17283119]

Shibata T, Yamada K, Watanabe M, Ikenaka K, Wada K, Tanaka K, Inoue Y. Glutamate transporter GLAST is expressed in the radial glia-astrocyte lineage of developing mouse spinal cord. J Neurosci. 1997; 17(23):9212–9. [PubMed: 9364068]

Sontheimer H, Minturn JE, Black JA, Waxman SG, Ransom BR. Specificity of cell-cell coupling in rat optic nerve astrocytes in vitro. Proc Natl Acad Sci U S A. 1990; 87(24):9833–7. [PubMed: 2263634]

Stallcup WB, Beasley L. Bipotential glial precursor cells of the optic nerve express the NG2 proteoglycan. J Neurosci. 1987; 7(9):2737–44. [PubMed: 3305800]

Warrington NM, Woerner BM, Daginakatte GC, Dasgupta B, Perry A, Gutmann DH, Rubin JB. Spatiotemporal differences in CXCL12 expression and cyclic AMP underlie the unique pattern of optic glioma growth in neurofibromatosis type 1. Cancer Res. 2007; 67(18):8588–95. [PubMed: 17875698]

Won CL, Oh YS. cAMP-induced stellation in primary astrocyte cultures with regional heterogeneity. Brain Res. 2000; 887(2):250–8. [PubMed: 11134613]

Zhu Y, Romero MI, Ghosh P, Ye Z, Charnay P, Rushing EJ, Marth JD, Parada LF. Ablation of NF1 function in neurons induces abnormal development of cerebral cortex and reactive gliosis in the brain. Genes Dev. 2001; 15(7):859–76. [PubMed: 11297510]

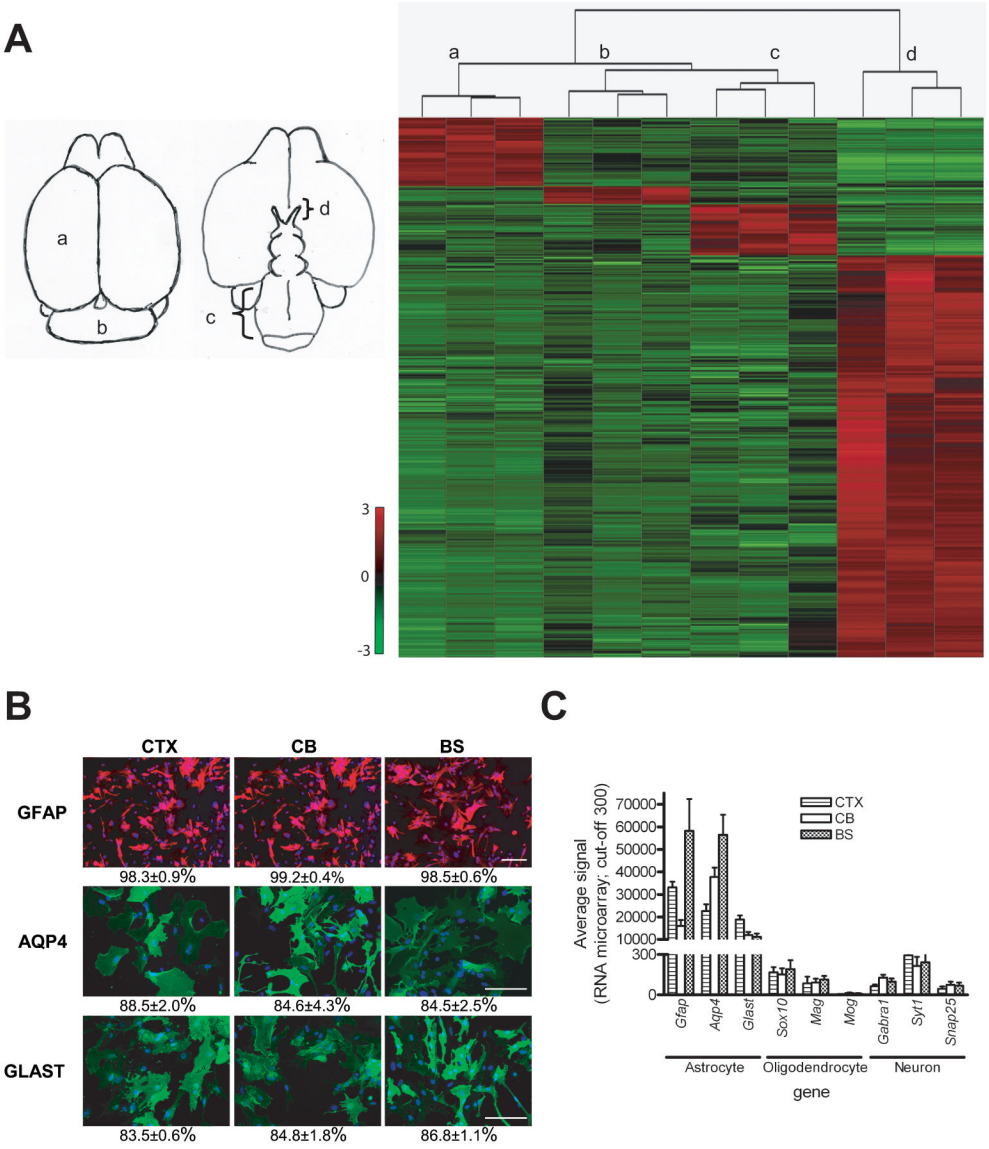

Figure 1. Identification of distinct gene expression patterns in astroglial cultures from different brain regions

(**A**) Hierarchical cluster analysis of astroglial cultures from different brain regions (as shown to the *left* of the heatmap) divides the samples into four distinct groups (**a**, neocortex; **b**, cerebellum; **c**, brainstem; **d**, optic nerve). Astroglial cells from optic nerve form an independent cluster separate from astroglial cells from neocortex, brainstem, and cerebellum. Gene expression data are filtered, z-score normalized (SD of 1 across all samples for each gene) to generate the heatmap. The expression level is shown representing standardized values from −3 (green, below the mean) to 3 (red, above the mean). The mean (0 value) is black. (**B**) Astroglial cells from neocortex (CTX), cerebellum (CB) and brainstem (BS) are GFAP+, AQP4+, and GLAST+. The percentages of positive staining for GFAP, AQP4 and GLAST in astrocytes from CTX, CB, and BS are > 98%, >84% and >83%, respectively. Scale bars=100 μm. (**C**) mRNA expression levels of astrocyte-, oligodendrocyte- and neuron-associated genes demonstrate that astroglial cells from all three regions express high levels of *Gfap*, *Aqp4* and *Glast* (astroglial-associated), but have almost undetectable levels of *Sox10*, *Mag* and *Mog* (oligodendroglial-associated) or *Gabra1*, *Syt1*

and *Snap25* (neuron-associated). The y-axis represents the level of gene expression as determined by MAS 5.0 with values <300 are scored as absent. Error bars represent the mean ±SEM.

A

Gene	Microarray (Fold Change)		Astrocytes RNA qPCR (Fold Change)				Neural stem cells RNA qPCR (Fold Change)				Brain tissues RNA qPCR (Fold Change)			
Neocortex	FC(CTX/BS)	FC(CTX/CB)	FC(CTX/BS)	*p*	FC(CTX/CB)	*p*	FC(CTX/BS)	*p*	FC(CTX/CB)	*p*	FC(CTX/BS)	*p*	FC(CTX/CB)	*p*
Atp1a2	6.00	10.19	9.67	*0.0002*	10.52	*0.0002*	5.38	*0.0673*	2.46	*0.1712*	0.66	*0.0785*	1.36	*0.0234*
Foxg1	76.58	44.68	29.27	*0.0007*	8.00	*0.0014*	21.43	*0.0005*	23.39	*0.0002*	186.08	*<0.0001*	104.41	*<0.0001*
Lhx2	52.91	52.53	21.35	*0.0011*	19.94	*0.0011*	2.75	*0.0417*	4.64	*0.0103*	4.07	*<0.0001*	26.76	*<0.0001*
Nr2e1	30.14	243.14	9.67	*<0.0001*	12.28	*<0.0001*	3.11	*0.0282*	4.68	*0.0127*	1.04	*0.6143*	0.65	*0.1097*
Cerebellum	FC(CB/BS)	FC(CB/CTX)	FC(CB/BS)	*p*	FC(CB/CTX)	*p*	FC(CB/BS)	*p*	FC(CB/CTX)	*p*	FC(CB/BS)	*p*	FC(CB/CTX)	*p*
En2	8.69	30.05	1.75	*0.0107*	22.57	*<0.0001*	1.13	*0.6480*	1.56	*0.2282*	2.01	*0.2004*	12.25	*0.0326*
Pax3	3.61	51.12	6.58	*0.0017*	69.27	*0.0007*	1.08	*0.8141*	1.52	*0.4106*	4.29	*<0.0001*	103.54	*<0.0001*
Ptn	6.41	2.35	4.97	*0.0007*	3.53	*0.0008*	0.99	*0.9456*	1.92	*0.0069*	0.70	*0.0010*	0.84	*0.0128*
Scn7a	14.10	9.43	5.90	*0.0134*	22.46	*0.0065*	1.43	*0.2544*	1.00	*0.9905*	1.44	*0.3213*	5.00	*0.0235*
Brainstem	FC(BS/CB)	FC(BS/CTX)	FC(BS/CB)	*p*	FC(BS/CTX)	*p*	FC(BS/CB)	*p*	FC(BS/CTX)	*p*	FC(BS/CB)	*p*	FC(BS/CTX)	*p*
Hoxa5	23.29	84.02	3.68	*0.0085*	2.54	*0.0282*	5.12	*0.0076*	2.92	*0.0513*	6.07	*0.0002*	22.41	*0.0001*
Hoxb3	8.43	41.13	5.08	*0.0158*	4.82	*0.0169*	4.18	*0.0044*	2.16	*0.0411*	2.16	*0.0497*	4.16	*0.0036*
Hoxb5	24.52	14.10	3.08	*0.0169*	3.29	*0.0169*	3.63	*0.0023*	2.30	*0.0517*	9.00	*0.0001*	29.75	*<0.0001*
Npy	3.75	5.09	5.90	*0.0150*	5.02	*0.0165*	2.27	*0.0039*	1.50	*0.1777*	10.01	*0.0002*	0.45	*<0.0001*

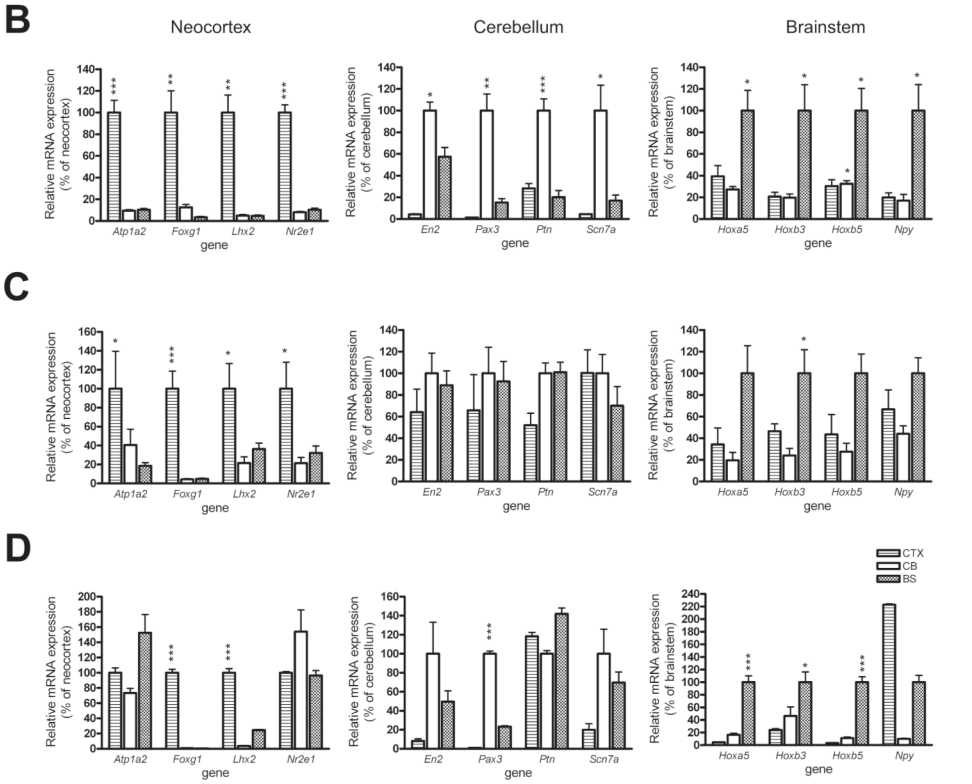

Figure 2. Validation of region-specific astroglial mRNA expression signatures by quantitative T-PCR

(**A**) Four representative candidate genes for each region were chosen for validation. The fold changes and *p* values calculated for each region are listed. The region-specific mRNA expression patterns of all 12 genes in astroglial cells confirmed the microarray results. Less consistent patterns of brain region-specific gene expression were observed in neural stem cells (NSCs) and brain tissues from these distinct brain regions. Graphic representation of the data presented in (**A**) are shown for independently-generated astroglial cell cultures (**B**), NSCs (**C**), and whole brain tissue (**D**). Error bars represent the mean±SEM. *, $p < 0.05$; **, $p < 0.01$; ***, $p < 0.001$.

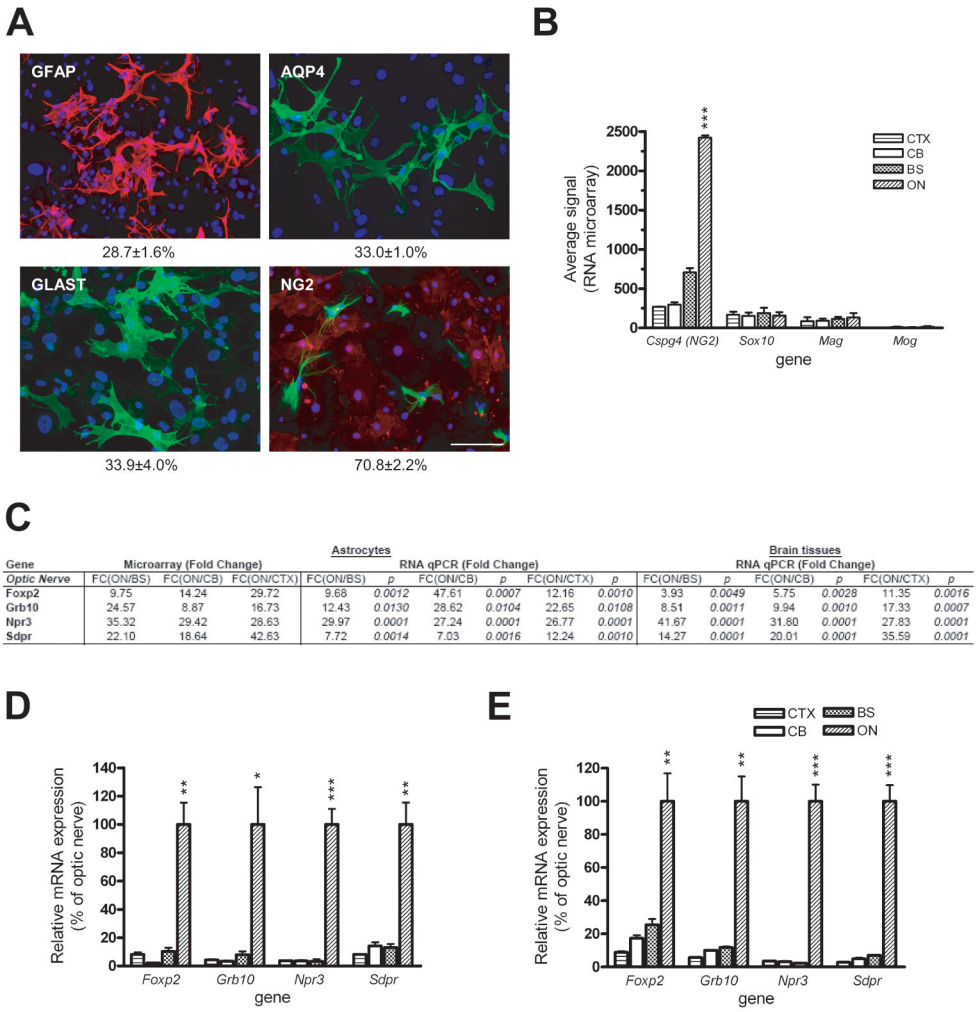

Gene	Microarray (Fold Change)			Astrocytes RNA qPCR (Fold Change)						Brain tissues RNA qPCR (Fold Change)					
Optic Nerve	FC(ON/BS)	FC(ON/CB)	FC(ON/CTX)	FC(ON/BS)	*p*	FC(ON/CB)	*p*	FC(ON/CTX)	*p*	FC(ON/BS)	*p*	FC(ON/CB)	*p*	FC(ON/CTX)	*p*
Foxp2	9.75	14.24	29.72	9.68	*0.0012*	47.61	*0.0007*	12.16	*0.0010*	3.93	*0.0049*	5.75	*0.0028*	11.35	*0.0016*
Grb10	24.57	8.87	16.73	12.43	*0.0130*	28.62	*0.0104*	22.65	*0.0108*	8.51	*0.0011*	9.94	*0.0010*	17.33	*0.0007*
Npr3	35.32	29.42	28.63	29.97	*0.0001*	27.24	*0.0001*	26.77	*0.0001*	41.67	*0.0001*	31.80	*0.0001*	27.83	*0.0001*
Sdpr	22.10	18.64	42.63	7.72	*0.0014*	7.03	*0.0016*	12.24	*0.0010*	14.27	*0.0001*	20.01	*0.0001*	35.59	*0.0001*

Figure 3. Optic nerve astroglial cells are a molecularly and genetically distinct glial subtype

(**A**) Only one-third of the cells in the optic nerve astroglial cell cultures expressed GFAP, AQP4 and GLAST by immunocytochemistry. Double-labeling with NG2 and GFAP revealed that ~70% of the cells are NG2+. Scale bars=100 μm. (**B**) RNA microarray analysis demonstrates markedly increased *Cspg4* (NG2) mRNA expression in ON astroglial cells with extremely low *Sox10*, *Mag* or *Mog* expression. The y-axis represents the level of gene expression as determined by MAS 5.0. Error bars represent the mean±SEM. (**C**) mRNA levels of the four representative ON astroglial cell-specific genes as determined by quantitative real-time RT-PCR. (**D & E**) Graphic representative of the data presented in (**C**) for independently-generated astroglial cell cultures (**D**) and whole brain tissue (**E**). Error bars represent the mean ±SEM. *, $p < 0.05$; **, $p < 0.01$; ***, $p < 0.001$.

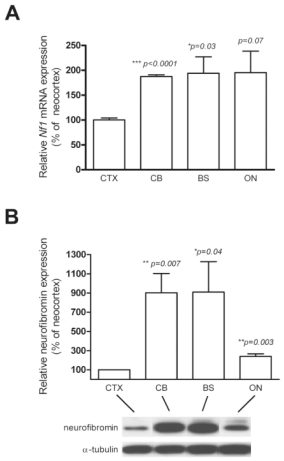

Figure 4. The *Nf1* gene is expressed at low levels in CTX astroglial cells

(**A**) *Nf1* mRNA expression is significantly lower in astroglial cells from CTX than in astroglial cells from the other brain regions as determined by quantitative real-time RT-PCR. (**B**) Neurofibromin expression is significantly reduced in astroglial cells from CTX relative to those from the other brain regions. α-tubulin was included as an internal loading control. Error bars represent the mean±SEM. *, $p < 0.05$; **, $p < 0.01$; ***, $p < 0.001$.

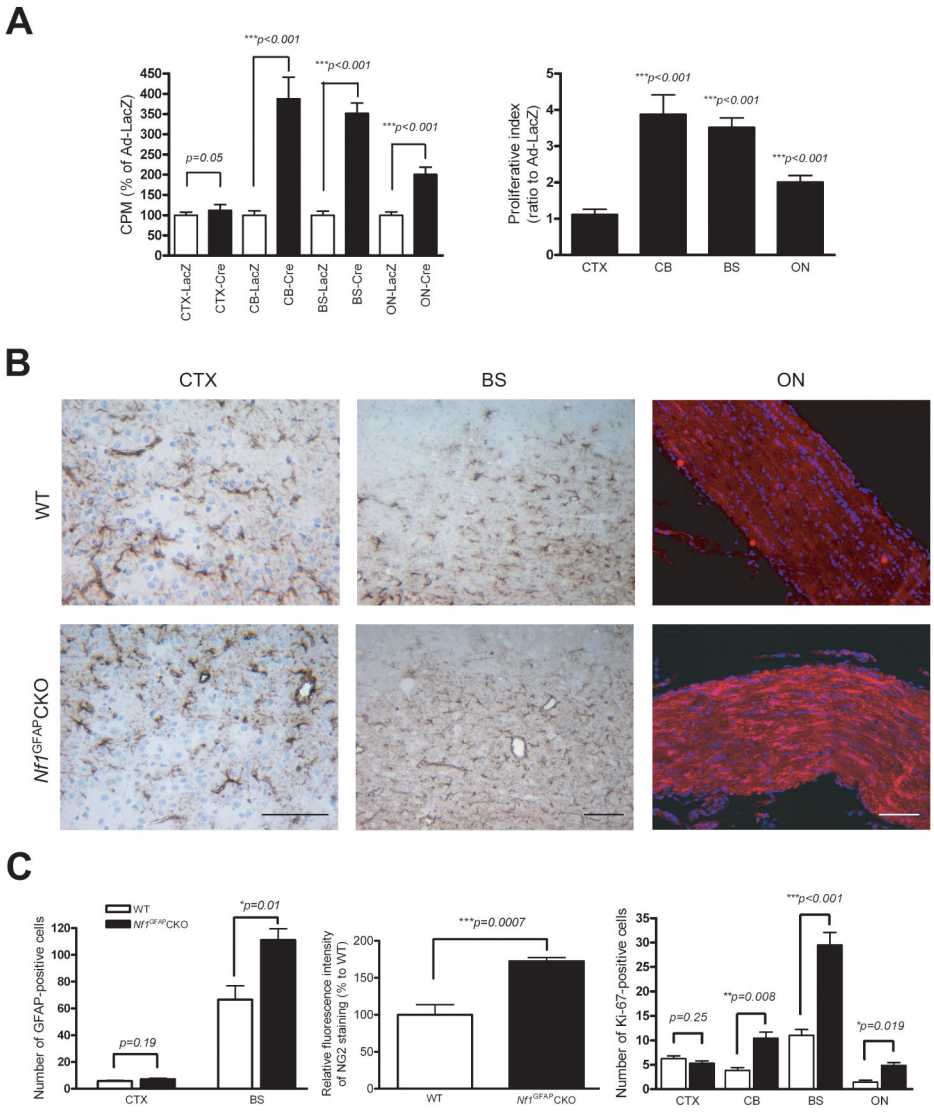

Figure 5. Neocortical astroglial cells exhibit no change in proliferation in response to *Nf1* inactivation *in vitro* or *in vivo*

(**A**) Whereas astroglial cells from CB, ON, and BS show increased proliferation in response to *Nf1* inactivation, no change in CTX astroglial cell proliferation was observed following neurofibromin loss, as determined by [^{3}H]-thymidine incorporation. (**B**) Increased numbers of GFAP-positive astrocytes are found in the CB and BS of *Nf1*^{GFAP}CKO mice compared to controls. Similarly, increased NG2 fluorescence intensity in *Nf1*^{GFAP}CKO mouse ON was observed relative to control mice. In contrast, no change in GFAP+ cell number was observed in the CTX of *Nf1*^{GFAP}CKO mice compared to controls. Scale bars=100 μm. (**C**) *Left*, quantification of the number of GFAP-positive cells in the BS and CTX of *Nf1*^{GFAP}CKO and control mice. *Middle*, quantitation of the relative NG2 fluorescence intensity in *Nf1*^{GFAP}CKO and control mouse optic nerves. *Right*, Ki-67 (MIB-1) quantitation reveals significantly increased numbers of Ki-67+ cells in the CB, BS and ON of *Nf1*^{GFAP}CKO mice compared to controls. No difference in the number of Ki67+ cells was observed in the CTX from *Nf1*^{GFAP}CKO mice compared to controls. Error bars represent the mean±SEM.

Table 1

Differential expression of tumor suppressor genes in astroglial cells

			RNA microarray (Fold Change)			
Probe set ID	**Gene Symbol**	**Gene Name**	**FC(BS/CTX)**	**FC(CB/CTX)**	**FC(ON/CTX)**	***p value***
Genes involved in familial cancer syndromes						
1458788_at	***Nf1***	**neurofibromatosis 1**	**1.97**	**2.25**	**4.55**	***0.0043***
1455252_at	*Tsc1*	tuberous sclerosis complex 1	1.35	1.27	1.88	*0.0012*
1452105_a_at	*Tsc2*	tuberous sclerosis complex 2	1.46	1.25	1.22	*0.1306*
1421820_a_at	*Nf2*	neurofibromatosis 2	1.65	1.02	1.65	*0.0005*
1422553_at	*Pten*	phosphatase and tensin homolog	0.85	1.15	1.79	*0.0004*
1427739_a_at	*Trp53*	transformation related protein 53	1.52	1.15	1.65	*0.0150*
1417850_at	*Rb1*	retinoblastoma 1	0.75	1.08	0.99	*0.0104*
1434708_at	*Vhlh*	von Hippel-Lindau syndrome homolog	0.63	0.83	0.46	*0.0014*
1420956_at	*Apc*	adenomatosis polyposis coli	0.92	0.88	0.48	*0.0082*
Other genes involved in tumorigenesis						
1416915_at	*Msh6*	mutS homolog 6 (*E. coli*)	0.83	1.08	1.29	*0.0036*
1417649_at	*Cdkn1c*	cyclin-dependent kinase inhibitor 1C (P57)	0.84	1.80	0.32	*0.0003*
1450140_a_at	*Cdkn2a*	cyclin-dependent kinase inhibitor 2A	0.37	1.37	1.10	*0.0047*
1417360_at	*Mlh1*	mutL homolog 1 (*E. coli*)	1.12	1.16	0.46	*0.0001*
1416988_at	*Msh2*	mutS homolog 2 (*E. coli*)	1.08	1.07	0.45	*0.0024*
1422486_a_at	*Smad4*	MAD homolog 4 (*Drosophila*)	0.64	0.95	0.64	*0.0001*
1428853_at	*Ptch1*	patched homolog 1	0.57	0.67	0.18	*0.0002*
1434045_at	*Cdkn1b*	cyclin-dependent kinase inhibitor 1B	0.35	0.54	0.51	*<0.0001*